Copyright © 2009 by ABCM

DETERMINATION OF TEMPERATURE MEASUREMENT POINTS USING GENERALIZED EXTREMAL OPTIMIZATION APPLIED TO FRICTION STIR WELDING PROCESS

Felipe Roman Centeno, felipe.centeno@tapme.com.br
Francis Henrique Ramos França, frfranca@mecanica.ufrgs.br
Departamento de Engenharia Mecânica – Universidade Federal do Rio Grande do Sul – UFRGS
Rua Sarmento Leite, nº 425, Bairro Cidade Baixa, Cep 90050-170, Porto Alegre, RS, Brasil

Abstract. *A methodology is proposed to determine the best locations of temperature measurements from which the unknown parameters of the friction stir welded (FSW) are to be determined from an inverse analysis. The methodology is based on the computation of the sensitivity of the measurement points, which measures how the temperatures are affected by the sought parameters. The study is based on numerical simulations of a three-dimensional conduction heat transfer process during friction stir welding of AA2195-T8 aluminum plates. For this purpose, a finite volume code was specifically developed to model the welding process, and the inverse analysis is treated as an optimization problem, which is solved with the Generalized Extremal Optimization (GEO) algorithm. The analysis is based on the temperatures artificially measured at several locations on the plate for different instant of time during the FSW pocess. This study shows that finding the locations with the highest temperature sensitivities can be an effective guide for a successful evaluation of the unknown parameter of the FSW process. This means that setting an inverse analysis based on the measurements of the temperatures on the most sensitive points are more likely to be successful.*

Keywords: *Friction stir welding, finite volume analysis, inverse analysis, numerical simulation, generalized extremal optimization.*

1. INTRODUCTION

Friction stir welding (FSW) is a relatively new, state-of-the-art solid state joining process. This metal joining technique is derived from the conventional friction welding. In a typical FSW, a rotating cylindrical pin tool is forced to plunge into the plates to be welded (i.e. workpiece) and moved along their contact line. During this operation, frictional heat that is generated by contact friction between the tool and workpiece softens the material. The plasticized material is stirred by the tool and forced to "flow" to the side and the back of the tool as the tool advances. As the temperature cools down, a solid continuous joint between the two plates is then formed. Because the highest temperature in the FSW process is lower than the melting temperature of the workpiece material, FSW yields fine microstructures, absence of cracking, low residual distortion and no loss of alloying elements, which are the main advantages of this solid phase process. Nevertheless, as in the traditional fusion welds, a softened heat affected zone and a tensile residual stress parallel to the weld are also formed.

The interest in FSW has increased significantly during the last years. The thermal modelling of this process has been a central part of the FSW research since the last 1990. Basically, there are three approaches that can be done: experimental, analytical, and numerical.

Analytical approaches were reported by Gould *et al.* (1998) and Schmidt *et al.* (2004). The first ones developed an analytical FSW model. That model was based on the Rosenthal equation and described the temperature field in a quasi-steady state on a semi-inifinite plate. The temperature field was generated by means of a moving heat source. The second work proposes an analytical expression which considers the contribution of both shoulder and pin to the heat generation during the welding process.

There are several researches related to the numerical study of FSW. It is important to mention that numerical studies are intimately related with experimental studies, since numerical codes are validated by means of experimental results. An important work was presented in Soundararajan *et al.* (2005), where the authors described the heat transfer between the workpiece and the backing plate, which is a difficult parameter to be evaluated both experimentally and numerically since it depends on the stress and the contact condutance.

Furthermore, there is a specific kind of numerical approach which is called as inverse problem. Inverse analyses make use of experimental data and numerical codes. Basically, an inverse problem can be described as the solution of a problem for which the typical outputs of the forward problem are used as inputs (temperatures in the present work), and their typical inputs are used as (unknown) outputs (heat sources and heat transfer coefficients).

An inverse problem was presented in the work of Chao *et al.* (2003), which tested different values of the heat source and of the heat transfer coefficient (between the workpiece and the backing plate) until the temperature values obtained numerically were equal to those obtained experimentally during the FSW process of aluminum AA2195 sheets. This procedure was called as "best fit". The same procedure was used in Zhu and Chao (2003), but the worpiece material considered was stainless steel 304L instead of aluminum, which turn the welding process more complex due to some material parameters such as thermal conductivity and stress strength. Another contribution on inverse analysis

was presented in Vilaça *et al.* (2006), in which the relation between the mechanical power imposed by the FSW machine and its amount that is transformed into friction heat was determined. In other words, they were able to provide the thermal efficiency of the FSW process. To perform this study, the authors measured temperatures in some locations on the workpiece, which were used as inputs of the inverse analisys, together with an analytical model of the heat transfer during the welding.

The present paper considers the solution of the transient three-dimensional heat conduction equation for the friction stir welding of AA2195-T8 aluminum plate using the finite volume analysis. Based on artificial measurements of temperature at different locations on the plate, an inverse analysis is carried out based on the optimization of an objective function. This function is defined as the error between the measured temperatures and the temperatures determined from the estimated parameters, which are: the heat input by the tool into the workpiece, the heat transfer coefficient between the workpiece and the support base, and the heat transfer coefficient between the workpiece and the environment. The optimization problem is solved with the Generalized Extremal Optimization (GEO) algorithm (Sousa *et al.*, 2003). Measurement data for the temperatures are artificially collected from exact values of temperatures obtained from a numerical solution performed by a given set of parameters, which are then perturbed with noises related to a specified standard deviation. In addition, a sensitivity study is accomplished in order to find the best positions to measure the temperatures during the welding process, since those values are used as input parameters of the inverse analysis.

An important topic in the present work is the analysis of the sensitivity related to the location of the temperature sensors. This sensitivity is calculated through the temperature variation in specific points on the workpiece during the welding, resulting from a perturbation on the unknown parameters: the heat source and heat transfer coefficients values. In this manner, the points with large sensitivity values present large variation in the temperature when the heat source or the coefficients are perturbed. As will be seen, this evaluation is very important for the inverse problem based on the use of the temperature values as inputs, and the heat source values as the main output data. Most previous works on estimation of unknown parameters in the FSW have been solved with "trial-and-error" method, but in the present study the inverse problem is treated as an optimization analysis, a much more flexible and robust technique.

2. PROBLEM DEFINITION AND NUMERICAL ANALYSIS

The modeled process considers the welding of two thin plates of aluminum AA2195-T8 using the friction stir welding (FSW) process. Each plate has 610 mm in length, 102 mm in width and 8.13 mm in thickness. The pin tool has a shoulder diameter of 25.4 mm. The geometry of the workpiece and the pin tool in a typical FSW is shown in Fig. 1. The pin tool starts at 12.7 mm away from the edge, and stops after translation of 584.6 mm along the weld line. The tool rotational speed is 240 rpm, and the tool translation velocity is of 2.36 mm/s; in this manner, the total welding time is 248 s. There is a pre-heat time (dwell period) of 5 seconds, in which the tool stands still at a distance of 12.7 mm from the border before it begins the translation. These parameters are the same used by Chao *et al.* (2003) in order to turn possible validate the code used in the present study.

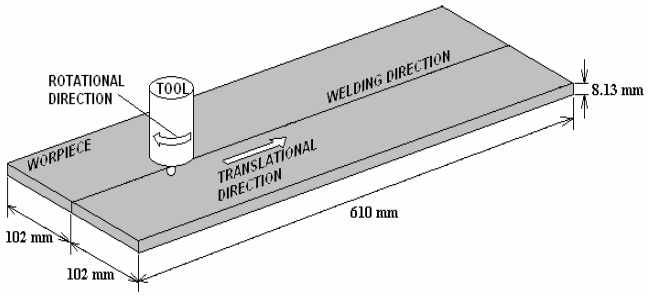

Figure 1. Geometry configuration of friction stir welding (FSW).

2.1. Finite volume method for transient heat transfer modelling

The transient temperature distribution T on the plate depends on the time t and the spatial coordinates (x, y, z), and is determined by the solution of the three-dimensional diffusion equation:

$$\rho c \frac{\partial T}{\partial t} = \frac{\partial}{\partial x}\left(k \frac{\partial T}{\partial x} \right) + \frac{\partial}{\partial y}\left(k \frac{\partial T}{\partial y} \right) + \frac{\partial}{\partial z}\left(k \frac{\partial T}{\partial z} \right) \tag{1}$$

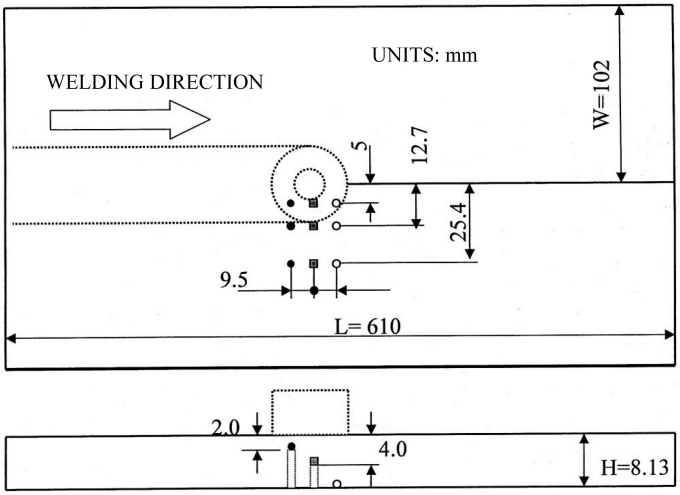

Figure 2. Locations of the temperature measurement (Chao *et al.*, 2003).

where k is the thermal condutivity, W/(m·K), c is the specific heat capacity, in J/(kg·K), and ρ is the specific mass of the material, in kg/m³. The friction stir welding is treated as a heat source moving along the line of the welding line. The heat produced by the friction between the pin tool shoulder and the plate is concentrated locally, and propagates into the other regions of the plates by conduction, in addition to the losses by convection on the boundaries and on the bottom surface. The total heat input, Q in W, can be evaluated by the following relation (Schmidt *et al.* 2004):

$$Q = \frac{2}{3}\pi\tau_{contact}\omega\left(R_{shoulder}^3 + 3R_{pin}^2 H_{pin}\right) \tag{2}$$

where $\tau_{contact}$ is the contact shear stress, in Pa, ω is the tool angular rotation speed, in rad.s^{-1}, $R_{shoulder}$ is the shoulder radius, in m, and R_{pin} and H_{pin} are pin tool radius and heigh, both in m. In addition, it is known the heat input obeys the following relationship

$$Q \approx \omega r \tau_{contact} A \tag{3}$$

where A is the contact area, in m², and r is the radial coordinate, in m. Neglecting the heat generated at the pin of the tool because it can be considered comparatively very small, e. g., in the order 2% of the total heat (Russell and Sheercliff, 1999), only the heat flux imposed by the tool shoulder is considered. In this manner, it is assumed that the heat flux q'' (in W/m²) imposed by the friction is distributed at the tool shoulder following the equation below:

$$q''(r) = \frac{3Qr}{2\pi R_{shoulder}^3} \tag{4}$$

The heat input Q (or, alternatively, q'') is unknown, its determination being one of the objectives of the present inverse analysis.

On the boundaries (surfaces) of the workpiece, convection heat transfer is responsible for heat loss to the ambient, which are given by:

$$q''_{conv} = h_{conv}\left(T - T_\infty\right) \tag{5}$$

where T_∞ is the environment temperature, in K, h_{conv} is the convection coefficient, in W/(m²·K). In this calculation, T_∞ = 298 K, h_{conv}= 30 W/(m²·K) are set to describe the process. Actually, the value of h_{conv} will be treated as an unknown and will be also determined from the inverse analysis. The heat loss from the bottom surface is due to heat conduction from the workpiece and support base plate, which depends on the geometry of the base as well as of the contact thermal resistance. An accurate evaluation of this heat loss is not a simple task, but experience has shown that it can be described by a rather simple relation that is similar to that used for the convection heat transfer, that is (Soundararajan *et al.*, 2005):

$$q_b^{"} = h_b (T - T_b) \tag{6}$$

where h_b is the heat transfer coefficient, in W/(m²·K), between the plate and the base, and T_b is the non-perturbed temperature of the base (that is, not affected by the contact with the plate), assumed here to be at the same value of the environment and surroundings, T_b = 298 K. The simple relation for the heat loss to the base requires the knowledge of the heat transfer coefficient between the plate and the supporting base, h_b. The objective of the inverse analysis is to determine h_b, in addition to the heat input Q and the convective coefficient h_{conv}, from measurements of the temperature.

Furthermore, in the numerical simulation of the FSW for AA2195-T8, it is assumed that the two plates are welded symmetrically during and after the welding. The welding line is along the symmetry line, and thus only one-half of the welded plate is modeled and the simetry surface is considered an adiabatic boundary.

In short, the boundary conditions are as follows:

- Under the tool shoulder (moving heat source): Equation (4).
- Simetry surface: Adiabatic boundary.
- Bottom surface: Equation (6).
- All other surfaces: Equation (5).

The finite volume method (FVM) code was developed, and then validated using the results reported in Chao *et al.* (2003). It is used a mesh as shown in Fig. 3, which has 122, 40 and 10 volumes in the x, y and z directions. The mesh is non-uniform in the y-direction: it has 32 volumes in the first 30 mm in the y-direction, and the remaining width of the plate is divided into 8 volumes, which obey a tangent-hiperbolic refinement equation. Besides, the temperature values are collected at the locations shown in Fig. 2, and the following values are used in the FVM code: Q = 1740 W, T_∞ = 298 K, T_b = 298 K, h_{conv} = 30 W/(m²·K), and h_b = 350 W/(m²·K) (the same as Chao *et al.*, 2003). The values of Q, h_{conv} and h_b will be outputs of the inverse analysis. The temperature profiles obtained with the FVM code developed in the this work show a very satisfactory comparison with the results presented in Chao *et al.* (2003).

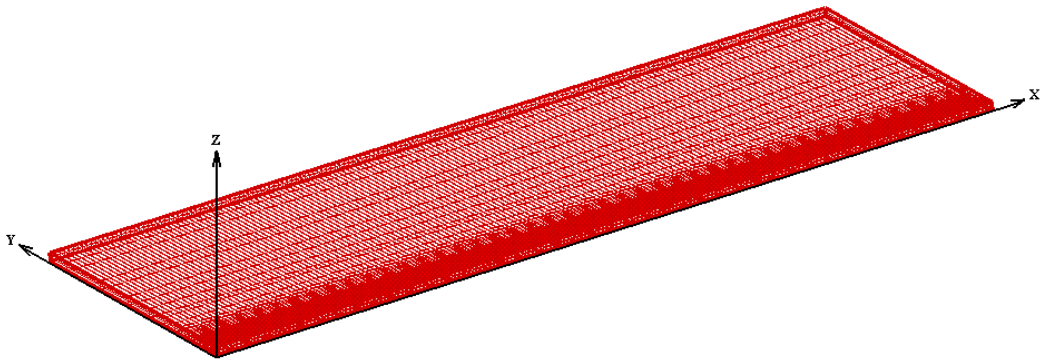

Figure 3. Finite volume method mesh.

In a grid independence study, several meshes were tested, and it was found that a mesh with 61×21×4 is refined enough to obtain good results, since using meshes more refined than this one generated nearly identical results, but the computational time increased significantly. This kind of study is very important because the FVM code will be run thousands of times during the optimization problem (inverse analysis).

The material properties of aluminum AA2195 used in the numerical solution was taken from Chao *et al.* (2003). The thermal properties are determined by the following relations (temperature T in °C):

$$k(T) = 89.643 + 0.201T \text{ , [W/m·°C]} \tag{7a}$$

$$c_p(T) = 131.643 + 0.118T \text{ , [J/kg·°C]} \tag{7b}$$

2.2. Sensitivity study related to the temperature acquisition locations

With the purpose of evaluating the best locations to install the temperature sensors, it was carried out a study to determine the sensitivity of the temperature measurements for several locations on the workpiece. The objective of this analysis is to find the best temperature measurement points, since these values are the inputs in the inverse analysis, while the heat source and the heat transfer coefficients values are the outputs. The points on the workpiece that present greater values of sensitivity should lead to the best results for the inverse analysis. S*ensitivity* is defined here as the rate in which the temperature changes with a variation in the heat source value or in the heat transfer coefficients. For instance, the sensitivity H_Q considers the temperature variation due to the variation on the heat source value, which can be expressed according to the following equation:

$$H_Q = \frac{Q}{T_{ref}} \left(\frac{\partial T}{\partial Q} \right)_i \tag{8}$$

where i represents a given temperature sensor, Q is the heat source, in W, and T_{ref} represents a reference temperature, in K, used to make the value of H_Q dimensionless (T_{ref} = 298 K). The sensitivity H_Q can be detemined numerically by central finite differences, according to:

$$H_Q = \frac{Q}{T_{ref}} \left(\frac{T(Q + \Delta Q) - T(Q - \Delta Q)}{2\Delta Q} \right)_i \tag{9}$$

ΔQ is the perturbation in the heat source value, which was chosen to be 10% in the present work, that is, 174 W.

The two other sensitivities that were studied in this work were: the one related to the convective heat transfer coefficient, H_{hconv}; and the sensitivity related to the heat transfer coefficient at the interface between the bottom surface of the plate and the base, H_{hb}. These two sensitivities are detemined similarly to H_Q, replacing Q by h_{conv} and h_b in equations (8) and (9). The increments on h_{conv} and h_b were also chosen to correspond to 10% of their reference values.

Table 1 shows the coordinates (x, y) that have the sensitivities computed. Centeno and França (2008) calculated sensitivities for three z-directions (0, 4.065 and 8.13 mm), but it was verified that the sensitivities values are very close for these three positions. So, in the present work it was only considered the z-direction 8.13 mm, which corresponds to the top surface of the workpiece. In a further experimental evaluation, this choice should simplify the installation of the temperature sensors. In order to clarify the data presented in Table 1, Figs. 4 and 5 illustrate the five sensor-assemblies A, B, C, D and E.

Table 1. Sensors locations subjected to the sensitivity analysis.

Sensor	(x; y)	Sensor	(x; y)	Sensor	(x; y)	Sensor	(x; y)	Sensor	(x; y)
A-1	(85; 13)	B-1	(135; 13)	C-1	(45; 13)	D-1	(45; 17)	E-1	(85; 13)
A-2	(85; 17)	B-2	(135; 17)	C-2	(65; 13)	D-2	(65; 17)	E-2	(65; 13)
A-3	(85; 21)	B-3	(135; 21)	C-3	(85; 13)	D-3	(85; 17)	E-3	(85; 17)
A-4	(85; 25)	B-4	(135; 25)	C-4	(105; 13)	D-4	(105; 17)	E-4	(65; 17)
A-5	(85; 29)	B-5	(135; 29)	C-5	(125; 13)	D-5	(125; 17)	E-5	(65; 21)

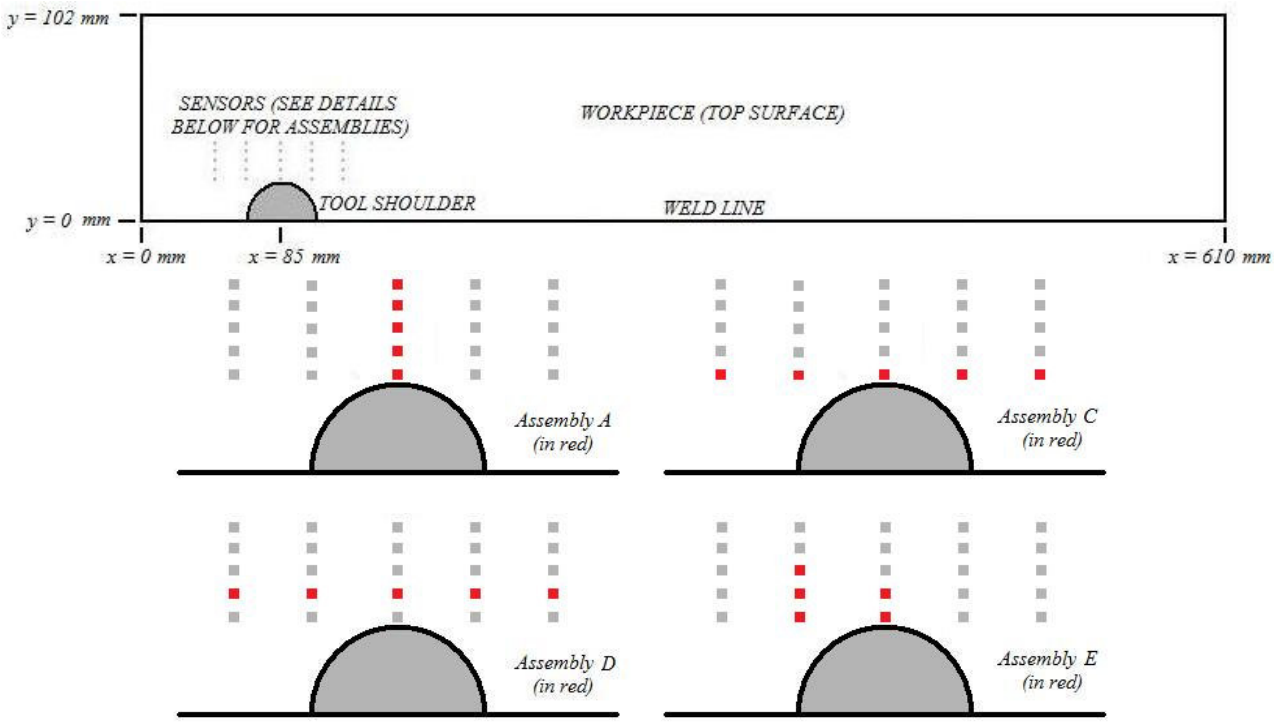

Figure 4. Temperature sensors for assemblies A, C, D and E (data acquisition when the heat source is at x = 85 mm).

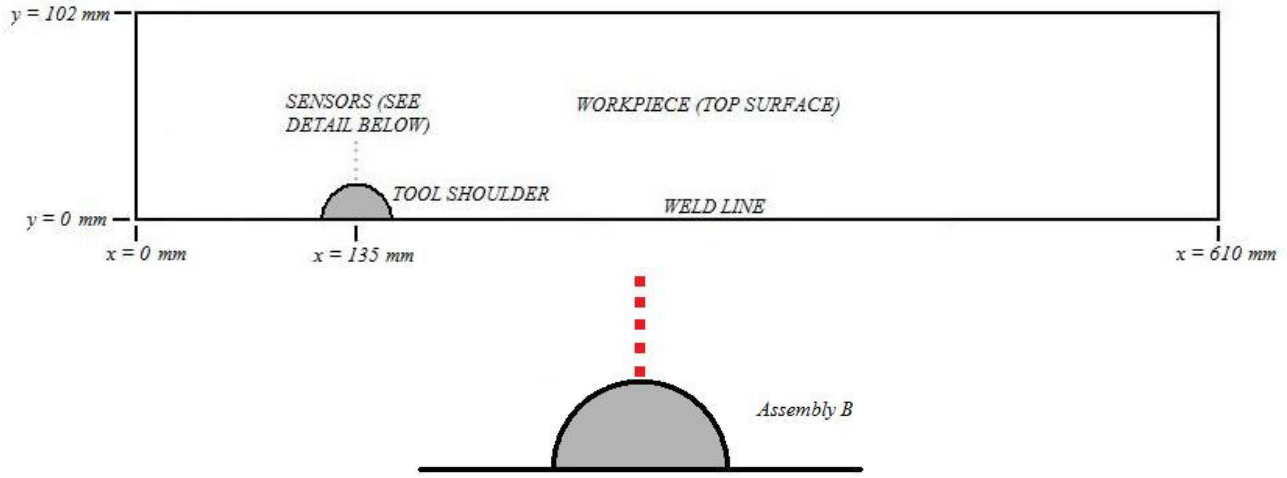

Figure 5. Temperature sensors for assembly B (data acquisition when the heat source is at x = 135 mm).

Note that assemblies A and B are perpendicular to the welding line, while assemblies C and D are parallel to it. Assembly E contains the sensors with the greatest sensitivities. The acquisition data instant for assemblies A, C, D, and E occurs when the heat source is at x = 85 mm; for assembly B, the heat source is at x = 135 mm. Table 2 shows the overall sensitivities values, computed as follows:

$$\sum_{i=1}^{5} H_{Q_i} = H_{Q_1} + H_{Q_2} + H_{Q_3} + H_{Q_4} + H_{Q_5} \tag{10}$$

Similar relations are used for H_{hb} and H_{hconv}. In Eq. (10), index i represents each temperature sensor, and the summation of the sensitivities is named as the overall sensitivity.

Table 2. Sum of the sensitivities values for the five sensors assemblies.

Assembly	**A**	**B**	**C**	**D**	**E**
ΣH_Q	35.729	36.376	30.449	27.289	42.227
ΣH_{hb}	4.288	4.856	4.372	4.275	5.496
ΣH_{conv}	0.307	0.347	0.332	0.331	0.403
$\Sigma H_Q + \Sigma H_{hb} + \Sigma H_{conv}$	40.324	41.579	35.153	31.895	48.126

From Table 2, one notes that the overall sensitivity related to the heat source is of the order 10^1, and for the heat transfer coefficient on the base and for the convective coefficient is of the order 10^0 and 10^{-1}, respectively, for all assemblies. This indicates that the most influent parameter on the temperatures is the heat source. This is especially interesting for an inverse analysis aiming at finding the heat source during the FSW from the measurement of the temperature. This because in general the higher the influence of a parameter on the measured quantities the more likely the inverse solution will be capable of recovering this parameter.

2.3. Generalized extremal optimization (GEO) method

The generalized extremal optimization (GEO) algorithm (Sousa *et al.*, 2003) is an evolutionary algorithm devised to improve the Extremal Optimization method (Boettcher and Percus, 2001) so that it could be easily applicable to virtually any kind of optimization problem. Both algorithms were inspired by the evolutionary model of Bak and Sneppen (1993). Following the Bak and Sneppen (1993) model, in GEO L species are aligned and for each species it is assigned a fitness value that will determine the species that are more prone to mutate. One can think of these species as bits that can assume the values of 0 or 1. Hence, the entire population would consist of a single binary string. The design variables of the optimization problem are encoded in this string that is similar to a chromosome in a genetic algorithm (GA) with binary representation.

To each species (bit) it is assigned a fitness number that is proportional to the gain (or loss) the objective function value has in mutating (flipping) the bit. All bits are then ranked from rank 1, for the least adapted bit, to N for the best adapted. A bit is then mutated (flipped) according to the probability distribution (1). This process is repeated until a given stopping criteria is reached and the best configuration of bits (the one that gives the best value for the objective function) found through the process is returned.

More details about this optimization method can be found in Sousa *et al.* (2003).

3. NUMERICAL EXPERIMENT - SOLUTION METHODOLOGY AND RESULTS

A simple, effective way of testing the proposed inverse analysis is to simulate the FSW process and, for given values of Q, h_b and h_{conv}, obtain the temperatures at the measurement locations shown in Tab. 1. Then, the inverse analysis is carried out to verify if the values of Q, h_b and h_{conv} can be correctly recovered. To consider a more realistic situation, for which the temperature measurements are affected by errors, the values of the temperatures obtained from the numerical simulations (for given values of Q, h_b and h_{conv}) will be perturbed by a noise according to a prescribed standard deviation σ. The objective is to evaluate how these noises can affect the estimation of Q, h_b and h_{conv}. The procedure of disturbing the numerical values of the temperatures will be denominated numerical-experimental values.

The procedure of the numerical-experimental method is outlined as follows:

1. Specify a value for the natural convection coefficient, h_{conv}. A reasonable guess is h_{conv} = 30 W/m²K;
2. Specify a value for the heat transfer coefficient at the bottom surface of the workpiece, h_b. A reasonable guess is h_b = 350 W/m²K;
3. Specify a value for the total heat input energy, Q, produced by the contact friction between the tool shoulder and the plates. A reasonable guess is Q = 1740 W;
4. Solve the three-dimensional differential equation (Eq. 1), under the previously described boundary conditions, using the finite volume numerical method. The solution of the resulting system of equations were accomplished with the TDMA method, setting a maximum relative temperature error between two subsequent iterations as 10^{-6};
5. Determine and store the temperature values, T_i, for the sensors locations shown in Tab. 1;
6. Generate random numbers ($rand_i$) between 0 and 1 (one random number for each sensor location);
7. Compute: ζ_i= 0.5-$rand_i$. With the value of ζ_i select the value of η_i from a table of integrals of the gaussian normal error function;
8. Choose the value of the standard deviation (σ): 0.0% (temperature reading without noise) and 3.0% (note that a tipical standard deviation value for infrared thermometers is 1.0%). It is considered that the standard deviation value associated to the temperature sensor is equal to 3σ, where σ is the standard deviation; in this manner the numerical measurement trust is of 99.73%.
9. Compute the value of the numerical-experimental temperatures: $T_i^{'} = T_i + \eta_i 3\sigma T_i$.

Steps 5 to 8 simulate measurement errors following a Gaussian distribution function with standard deviation of σ. It must be emphasized that the standard deviation values, σ, must be multiplied by T_i in step 9 because they are present in step 8 as percentual values, thus the value of (σT_i) on step 9 is the standard deviation value in K. In addition, the value of (σT_i) is multiplied by 3 in order to get a larger trust interval (99.73%). Table 3 shows the numerical-experimental temperatures for each temperature sensor, $T_i^{'}$ (in K).

Table 3. Numerical-experimental temperature values, $T_i^{'}$ (in K).

3σ = 0.0%									
Sensor	$T_i^{'}$ (in K)	Sensor	$T_i^{'}$ (in K)	Sensor	$T_i^{'}$ (in K)	Sensor	$T_i^{'}$ (in K)	Sensor	$T_i^{'}$ (in K)
A-1	578.54	B-1	581.744	C-1	490.91	D-1	479.933	E-1	578.54
A-2	522.942	B-2	526.358	C-2	550.398	D-2	525.066	E-2	550.398
A-3	480.71	B-3	484.287	C-3	578.54	D-3	522.942	E-3	522.942
A-4	447.232	B-4	450.923	C-4	392.603	D-4	380.268	E-4	525.066
A-5	420.283	B-5	424.046	C-5	319.24	D-5	317.543	E-5	499.228
3σ = 3.0%									
Sensor	$T_i^{'}$ (in K)	Sensor	$T_i^{'}$ (in K)	Sensor	$T_i^{'}$ (in K)	Sensor	$T_i^{'}$ (in K)	Sensor	$T_i^{'}$ (in K)
A-1	574.234	B-1	577.392	C-1	487.839	D-1	477.017	E-1	574.234
A-2	513.724	B-2	528.865	C-2	553.143	D-2	527.56	E-2	553.143
A-3	473.051	B-3	476.496	C-3	574.234	D-3	513.724	E-3	513.724
A-4	455.536	B-4	459.403	C-4	398.302	D-4	385.378	E-4	537.082
A-5	418.782	B-5	422.507	C-5	318.769	D-5	317.09	E-5	496.922

4. INVERSE ANALYSIS - SOLUTION METHODOLOGY AND RESULTS

Once the numerical-experimental temperatures are obtained, the thermal-optimization analysis (inverse problem) is carried out following the steps below:

1. Specify the range of the parameters which will be optimized:
   a. Total heat generated by friction: 200 W $\leq Q \leq$ 2000 W;
   b. Heat transfer coefficient at the bottom surface: 100 W/m²K $\leq h_b \leq$ 500 W/m²K;
   c. Convective heat transfer coefficient: 10 W/m²K $\leq h_{conv} \leq$ 50 W/m²K;
2. Specify the number of function evaluations: *NFE* = 2000,
3. Specify the parameter τ: τ = 1.25;
4. Specify the objective function as $F(Q,h_b,h_{conv}) = \left[\sum_{i=1}^{I}\left(T_i^{'} - T_{i,cal}\right)^2\right]^{1/2}$, where $T_{i,cal}$ is the temperature computed in point *i* for given values of Q, h_{conv} and h_b, and I is equal to number of measurement points (I = 5);
5. Run GEO and obtain the best estimates for Q, h_{conv} and h_b.

It should be noted that the number of function evaluations (*NFE*) is equal to the number of times that the finite volume code is run, which means that the finite volume code must be as efficient as possible in order to accelerate the optimization process, which is time consuming due to its evolutionary nature.

The number of function evaluations (NFE) was set as 2000 in step 2 above, since the results related to the relative errors for the optimized values of Q, h_b and h_{conv} do not decrease beyond this value. NFE ranged from 500 to 100000.

Centeno and França (2008) showed that the use of τ = 1.25, used in step 3, is a good value for parameters estimation in FSW, which is confirmed in the present work.

Table 4 shows the results obtained from the inverse analysis for Q_{best}, $h_{b,best}$ and $h_{conv,best}$ for the five sensors assemblies, and their relative errors in parenthesis. Although all assemblies showed satisfactory results, with relative errors ranging from 1.206 to 4.353% for Q_{best}, assemblies A and E led to the best results. The main objective of the present analysis is to determine the heat source in the FSW, so it should be observed that assembly A presented the best results, with relative error related to the heat source of 1.206%, although this assembly did not have the highest sensitivity H_Q. On the other hand, assembly E had the highest H_Q, and the relative relative error related to the heat source was of 1.221%, slightly higher than that for assembly A. In this manner, assembly A can be considered the best location to install the temperature sensors to recover the heat input from the inverse analysis. This can be explained by the fact that, in comparison to assembly E, the sensors in assembly A experience a wider range of temperatures, as show in Table 3, which also has importance in the recovery of the unknown heat source from an inverse solution.

Centeno and França (2008) reported relative error for Q_{best} of 0.424% for an uncertainty of 1.0%, obtained for an assembly parallel to the weld line (similar to assembly C in the present work) with ten sensors. It must be emphasized that the present study considered only five sensors in each assembly, and the relatively large uncertainty of 3.0%, which turns the inverse analysis more difficulty due to higher inputs noises and less impulse inputs to feed the analysis.

Analyzing the results in Table 4, one notes that the smallest errors in the estimation of the heat source results from its greater influence on the temperature distribution on the workpiece, when compared to the influence of the heat transfer coefficients. It is emphasized that these results are in accordance with the sensitivity results shown in Section 2.2 (Table 2), since the sensitivity for the heat source is much larger than those for the heat transfer coefficients. Since the main objective of the present analysis is to determine the heat source in the FSW, not the heat transfer coefficients, the proposed inverse solution can be considered satisfactory despite some large errors on the heat transfer coefficients.

Table 4. Heat source Q_{best} (W), heat transfer coefficient at bottom surface, $h_{b,best}$ (W/(m².K)), and convective heat transfer coefficient, $h_{conv,best}$ (W/(m².K)), for uncertainties of 0.0% and 3.0%.

Assy.	Uncertainty of 0.0%			Uncertainty of 3.0%		
	Q_{best} (W)	$h_{b,best}$ (W/(m².K))	$h_{conv,best}$ (W/(m².K))	Q_{best} (W)	$h_{b,best}$ (W/(m².K))	$h_{conv,best}$ (W/(m².K))
A	1736.328 (0.211 %)	324.928 (7.160 %)	49.895 (66.300 %)	1719.010 (1.206 %)	351.680 (0.480 %)	29.062 (3.100 %)
B	1725.762 (0.818 %)	323.291 (7.631 %)	37.500 (25.000 %)	1692.384 (2.736 %)	313.270 (10.490 %)	21.832 (27.230 %)
C	1725.664 (0.824 %)	314.348 (10.200 %)	49.113 (63.700 %)	1664.260 (4.353 %)	308.008 (11.990 %)	28.750 (4.170 %)
D	1722.266 (1.019 %)	308.942 (11.730 %)	49.967 (66.600 %)	1664.482 (4.340 %)	308.493 (11.860 %)	29.311 (2.290 %)
E	1746.876 (0.395 %)	368.689 (5.34 %)	24.958 (16.800 %)	1718.752 (1.221 %)	352.311 (0.660 %)	28.205 (6.000 %)

5. CONCLUSIONS

This paper considered the estimation of governing parameters of the friction stir welding (FSW) of an aluminum AA2195-T8 plate. The estimation was carried out by means of an optimization problem, in which the objective function corresponded to a measure of the error between the numerically-measured temperatures and the temperatures computed for each estimated value of the heat source, and the unknown heat transfer coefficients. The time-dependent temperature distribution on the plate was determined by the solution of the three-dimensional transient diffusion equation, which was solved by the control-volume method. The minimization of the objective function was accomplished with the aid of the Generalized Extremal Optimization (GEO) algorithm. The estimations of the heat source input in the tool shoulder, and of the heat transfer coefficients were carried out from the measurement of several temperatures located on the top surface of the plate. To simulate real-data measurements, the temperature inputs, obtained from a simulation based on specific values of the heat input and of the heat transfer coefficients, were perturbed with noises according to a standard deviation of the measurement procedure. In order to obtain the best locations of the temperature sensors, it was performed a sensitivity study. This study consisted of evaluating, in several places on the workpiece, the variations on the temperatures with variations on the sought parameters. The overall sensitivity for the heat source was of the order 10^2, and for the heat transfer coefficient on the base and for the convective coefficient was of the order 10^1 and 10^{-1}, respectively. Overall, the proposed methodology was capable of providing a satisfactory estimation for the three unknown parameters, especially for the heat source. The small error in the estimative of the heat source results from its greater influence on the temperature field and, therefore, greater sensitivity. Also, these results can be considered an advance when compared to the results presented in Centeno and França (2008), which considered a higher number of sensors and smaller measurement errors.

6. ACKNOWLEDGEMENTS

The second author thanks CNPq for research grants 304535/2007-9. Both authors thank Dr. Fabiano Luis de Sousa (INPE) for providing the GEO algorithm code.

7. REFERENCES

Bak, P. and Sneppen, K., 1993, "Punctuated Equilibrium and Criticality in a Simple Model of Evolution", Physical Review Letters, Vol. 71, Number 24, pp. 4083-4086.

Boettcher, S. and Percus, A.G., 2001, "Optimization with Extremal Dynamics", Physical Review Letters, Vol. 86, pp. 5211-5214.

Centeno, F. R., França, F. H. R., 2008, "Application of the Inverse Analysis to the Heat Transfer in Friction Stir Welding", 12th Brazilian Congress of Thermal Engineering and Sciences, Belo Horizonte, MG, Brazil.

Chao Y.J., Qi X., and Tang W., 2003, "Heat transfer in friction stir welding - experimental and numerical studies", ASME J. Manuf. Sci. Eng. 125, pp. 138-145.

Gould J., and Feng Z., 1998, "Heat flow model for friction stir welding of aluminum alloys", J. Mater. Process. Manuf. Sci. 7, pp. 185–194.

Russell, M. J., Sheercliff, H. R., 1999. "Analytic Modelling of Microstructure Development in Friction Stir Welding", 1st International Symposium on Friction Stir Welding, Thousand Oaks, CA, USA.

Schmidt, H., Hattel, J., Wert, J., 2004. "An Analytical Model for the Heat Generation in Friction Stir Welding", Modelling and Simulation in Materials Science and Engineering, vol. 12, pp. 143 – 157.

Soundararajan, V., Zekivic, S., Kovacevic, R., 2005. "Thermo-mechanical Model with Adaptive Boundary Conditions for Friction Stir Welding of Al 6061", International Journal of Machine Tools & Manufacture, vol. 45, pp. 1577 - 1587.

Sousa, F.L., Ramos, F.M., Paglione, P., and Girardi, R. M., 2003, "New Stochastic Algorithm for Design Optimization", AAIA Journal, Vol. 41., No. 9., pp. 1808-1818.

Vilaça, P., Quintino, L., dos Santos, J. F., Zettler, R., Sheikhi, S., 2006. "Quality Assessment of Friction Stir Welding Joints via an Analytical Thermal Model, iSTIR", Materials Science and Engineering, vol. 445, pp. 501 – 508.

Zhu, X. K., Chao, Y. J., 2003. "Numerical Simulation of Transient Temperature ans Residual Stresses in Friction Stir Welding of 304L Stainless Steel", Journal of Materials Processing Technology, vol. 146, pp. 263 – 272.

8. RESPONSIBILITY NOTICE

The authors are the only responsible for the printed material included in this paper.